Analysis of a Concentrated Winding Induction Machine for Adjustable Speed Drive Applications Part 1 (Motor Analysis)

Hamid A. Toliyat
Student Member, IEEE
Thomas A. Lipo
Fellow, IEEE
University of Wisconsin-Madison
1415 Johnson Drive
Madison, WI 53706

J.Coleman White
Life Fellow, IEEE
Electric Power Research Inst.
3412 Hillview Ave.
Palo Alto CA 94303

Keywords: Concentrated Windings, Adjustable Speed Drive, Induction Machines

Abstract - The performance of multiphase concentrated winding induction machines specifically designed for operation with static power converters is investigated. The winding distributions are intentionally rectangular to better accommodate the rectangular wave forms of solid state inverters. Equations which define the transient as well as steady state behavior including the computation of all machine inductances are derived. Equations for calculation of terminal voltages and electromagnetic torque have also been modified to account for non sinusoidal air gap flux distributions.

1. Introduction

The design of conventional synchronous and asynchronous machines aims for a perfect sinusoidal winding distribution on the stator and rotor in order to minimize space harmonics. Except for slot harmonics, the resultant air-gap field is therefore nearly sinusoidally distributed so that during steady state, essentially only the desired average (dc) torque occurs in the machine when excited from a balanced supply. With the advent of controlled semiconductors, associated converter development has provided the means to produce motor current waveforms of nearly any desired shape. Nearly exclusive attention has, however, been directed towards development of solid state inverters which minimize the harmonic content of the voltages applied to ac machines equipped with conventional distributed windings. The objective of such development is to produce a rotating field having a minimum of time harmonics and approach the equivalent of a balanced sine wave supply. In effect, the sinusoidal winding distribution ensures that the counter EMF of the machine remains nearly sinusoidal despite the non-sinusoidal impressed voltage. Hence the harmonic currents that flow are nearly entirely loss components and not torque producing components.

Within the variable-speed drive family, the squirrel-cage induction motor fed by a pulse-width-modulated inverter continues to dominate. This robustly constructed motor is the machine of choice for most low cost as well as for difficult environmental conditions. These machines have typically been designed to operate from fixed frequency, fixed voltage supplies. Induction machines of such conventional design have also been widely used in variable speed drives. In such cases solid state inverters have provided flexibility, allowing satisfactory, if not optimum, operation of the machine over a wide speed range. Two types of inverters have emerged suitable for powering induction machine drives, the pulse width modulated (PWM) voltage source inverter and the auto-sequentially commutated current source inverter (CSI).

In order to achieve the desired performance, current flow in the motor phases must typically be controlled to assume a prescribed waveform. Probably the most suitable converter structure for such a requirement is the pulse-width-modulated or PWM voltage source inverter. To reduce the harmonic content of the inverter voltage waveforms, modulation techniques were adopted in the 1960s to eliminate selected low order harmonics [1,2]. As the switching frequency of devices increased, it became possible to modulate the inverter's output voltage waveform at a much higher frequency than could previously be achieved. This allowed the inverter output to be synthesized in such a manner that virtually all the low order harmonics and the consequent losses associated with them are eliminated. With a suitably distributed motor winding, such a supply established a smoothly rotating magnetic field with a spatial distribution approximating a sinusoid.

91 WM 051-3 EC A paper recommended and approved by the IEEE Electric Machinery Committee of the IEEE Power Engineering Society for presentation at the IEEE/PES 1991 Winter Meeting, New York, New York, February 3-7, 1991. Manuscript submitted August 27, 1990; made available for printing November 30, 1990.

2. Historical Background

With the development of solid-state power converters, the range of application of ac machines has expanded enormously as a result of the ability of these machines to operate with a variable frequency inverters and therefore at a variable speed. In general, motor designers continue to emphasize the design of conventional three phase, sinusoidally fed induction machines. However, progress has already been made on machine structures that deviate from these cardinal rules.

It is the nature of inverters, by virtue of their inherent discrete switching, to impress rectangular voltage or current pulses on the motor rather than sinusoidal quantities. Instead of directing development work exclusively into the design of inverters with quasi-sinusoidal voltage or current output, it appears useful and practical to consider the design of new types of induction machines having winding distributions which are more compatible with the switching nature of the supply. If the machine is wound with concentrated rather than pitched and distributed windings, the air gap flux could, if desired, be made to take on a rectangular rather than sinusoidal shape. In a machine with a sinusoidal air-gap flux distribution, only a small part of the active iron core is near saturation at any one time. Only in the small region where the flux density wave is maximum is the iron saturated to the desired extent, while the rest of the iron does not reach full saturation. The iron would be utilized better if the air-gap flux density would have a more nearly rectangular form. The power density of the machine could clearly be improved if the stator and rotor flux density together result in a nearly rectangular air-gap flux density wave traveling at constant angular velocity. The peak fundamental component of such a square wave is $4/\pi$ times or 127% as large as that of a comparable sine distribution having the same peak flux density. Further enhancement of the torque capability beyond $4/\pi$ is available in principle through rotor interaction with higher order space harmonics of the air-gap flux density wave [3].

A study of the behavior of a synchronous machine with a quasi-rectangular flux distribution was first carried out by Lipo and Wang [3,4]. In this paper the authors considered the variation in power output of a machine when the flux distribution is changed from a sinusoidal shape. The criteria selected were to keep both the r.m.s. current in the windings and the total air-gap flux constant. Since the r.m.s. currents are the same and the winding resistances are assumed to be constant, copper losses are essentially the same. Various flux waveshapes were considered. With these criteria the shape which was found to give the highest output was a quasi-rectangular shape with an active span of 120 electrical degrees per pole. The increase in power output was found to be 15% over that for a machine with sinusoidally distributed flux. Recently [5], a slightly decreased pole arc of 115 degrees was proposed as a means to further increase torque output.

Recently Dente [6] has suggested that the concentrated winding principle, applied successfully to synchronous machines, may also be possible for induction machines. Specifically he shows approximately a 10% decrease in losses for the same output power when a 9 phase induction motor is operated near its rated condition. Gosden [7] analyzed induction machines with different numbers of phases and concluded that a theoretical increase in torque of about 17% can be achieved with a 12 pulse, 6 phase system for a given machine frame size. These two studies serve to further substantiate and quantify the potential of enhancing the power density of induction machines.

In 1985 Weh and Schroder [8] examined the increase in the tangential force density for a rectangular flux synchronous machine supplied by seven phases. In the ideal case they found that for the same peak values of flux and current, the force density increased by a factor of two over a machine with sinusoidally distributed flux. However, flux leakage and saturation reduced this to about 1.75 times for the practical case. The study did not take into account the higher rms currents in the windings nor the larger yoke dimensions required to carry the higher total flux.

3. Goals of This Study

The overall goal of this study is to investigate the design of a special purpose induction machine for use as a variable speed drive, which abandons the conventional sinusoidally wound machine structure for alternative winding strategies that realize trapezoidal or rectangular field distributions which can readily be complemented by programming the current from an inverter source. While work on this problem has progressed sporadically, a clear indication of benefits that can be attained with non-sinusoidally wound induction machines has yet to appear. One of the chief stumbling blocks to such work has specifically been the lack of a suitable induction motor machine model for simulating both transient and steady state behavior of non-sinusoidally wound machines. The development of such a model has been a major contribution of the work contained in this paper.

Secondly, it remains unclear whether an increased number of phases will actually increase the power density in an induction machine. Also, if increased power density is possible, the question of selecting the optimum phase number and optimum winding distribution remains unanswered. Part II of this paper sheds light on these questions for the determination of the degree of improvement offered by these many alternatives.

4. Modelling of Induction Machines with Nonsinusoidally Distributed Windings

The so-called d-q model of induction machines is based on the assumption that the "stator windings are sinusoidally distributed". In other words, in effect, all harmonics of the stator winding distribution except for the fundamental are neglected. While a valid approximation for conventional machines, replacement of concentrated windings (square wave windings) with equivalent sinusoidal windings is clearly not valid if reasonable approximations of the motor voltage and current wave shapes are to be obtained. Hence the analysis of this type of machine becomes complicated due to the fact that the usual transformations no longer yield a simplification in the model. In this study we are particularly interested in these harmonics. Consequently, the coupled magnetic circuit approach is used to derive a new mathematical model of a general concentrated winding machine with m phase stator windings, n rotor bars (m-n winding machine) . The work to follow can be considered as an extension of Ref. 9 in which stator windings having only sinusoidal distributions were considered The machine is simulated in the so-called natural frame of reference. That is, the machine is simulated in terms of the actual physical rather than transformed or equivalent variables. The model is applicable to both squirrel cage and phase wound rotors and also for cage rotors with non-integral numbers of rotor bars per stator pole-pair.

5. Equations for an m-n Concentrated Winding Machine

Consider initially a general m-n winding machine with the following assumptions,

- •negligible saturation
- •uniform air-gap
- •m identical stator windings with axes of symmetry
- •n uniformly distributed cage bars or identical rotor windings with axes of symmetry such that even harmonics of the resulting spatial winding distribution are zero
- •eddy current, friction, and windage losses are neglected
- •inverter switching devices are ideal (zero impedance when on, infinite impedance when off)
- •the dc link power supply is an ideal current source.

The cage rotor can be viewed as n identical and equally spaced rotor loops. For example, the first loop may consist of the 1st and (k+1)th rotor bars and the connecting portions of the end rings between them, where k is any arbitrarily chosen integer ($1 \le k \le n$) and the second loop consists of the 2nd and (k+2)th rotor bar and the connecting portions of the end rings between them and so on.

6. Stator Voltage Equations

The voltage equations for the stator loops can then be written

$$V_s = R_s I_s + \frac{d\Lambda_s}{dt} \tag{1}$$

where

$$\Lambda_s = L_{ss} I_s + L_{sr} I_r \tag{2}$$

and

$$I_s = \left(i_1^s \; i_2^s \ldots\ldots\ldots\ldots i_m^s\right) t \tag{3}$$

$$I_r = \left(i_1^r \; i_2^r \ldots\ldots i_n^r\right) t \tag{4}$$

$$V_s = \left(v_1^s \; v_2^s \ldots\ldots\ldots\ldots v_m^s\right) t \tag{5}$$

The matrix R_s is a diagonal m by m matrix given by

$$R_s = r_s I \tag{6}$$

where the matrix I is an m by m identity matrix and r_s is the resistance of each coil assuming all coils are similar.

Due to conservation of energy the matrix L_{ss} is a symmetric m by m matrix of the form

$$L_{ss} = \begin{pmatrix} L_{11}^s & L_{12}^s & \ldots\ldots\ldots\ldots & L_{1m}^s \\ L_{21}^s & L_{22}^s & \ldots\ldots\ldots\ldots & L_{2m}^s \\ \vdots & \vdots & & \vdots \\ \vdots & \vdots & \ldots\ldots\ldots\ldots & \vdots \\ L_{m1}^s & L_{m2}^s & \ldots\ldots\ldots\ldots & L_{mm}^s \end{pmatrix}, \tag{7}$$

The mutual inductance matrix L_{sr} is an m by n matrix comprised of the mutual inductances between the stator coils and the rotor loops.

$$L_{sr} = \begin{pmatrix} L_{11}^{sr} & L_{12}^{sr} & \ldots\ldots\ldots\ldots & L_{1n}^{sr} \\ L_{21}^{sr} & L_{22}^{sr} & \ldots\ldots\ldots\ldots & L_{2n}^{sr} \\ \vdots & \vdots & & \vdots \\ \vdots & \vdots & \ldots\ldots\ldots\ldots & \vdots \\ L_{m1}^{sr} & L_{m2}^{sr} & \ldots\ldots\ldots\ldots & L_{mn}^{sr} \end{pmatrix} \tag{8}$$

Since the inductance matrix L_{ss} is constant whereas L_{sr} varies with the position of the rotor, the second term of Eq. (1) can be written as

$$\frac{d\Lambda_s}{dt} = L_{ss}\frac{dI_s}{dt} + \frac{dL_{sr}}{dt} I_r + L_{sr}\frac{dI_r}{dt} \tag{9}$$

The second term in the above equation can be written using the chain rule as

$$\frac{dL_{sr}}{dt} I_r = \frac{dL_{sr}}{d\theta_{rm}} \frac{d\theta_{rm}}{dt} I_r \tag{10}$$

Defining rotor mechanical speed as

$$\omega_{rm} = \frac{d\theta_{rm}}{dt} \tag{11}$$

then

$$\frac{dL_{sr}}{dt} I_r = \omega_{rm} \frac{dL_{sr}}{d\theta_{rm}} I_r \tag{12}$$

Therefore, Eq. (9) can typically be written in the form,

$$\frac{d\Lambda_s}{dt} = L_{ss}\frac{dI_s}{dt} + \omega_{rm}\frac{dL_{sr}}{d\theta_{rm}} I_r + L_{sr}\frac{dI_r}{dt} \tag{13}$$

7. Rotor Voltage Equations

The representation of an induction machine with a cage rotor is fundamentally the same as one with a phase wound rotor where it is assumed that the cage rotor can be replaced by a set of mutually coupled loops. One particular advantage of this approach is that it is also applicable to cage rotors with non-integral numbers of rotor bars per pole-pair.

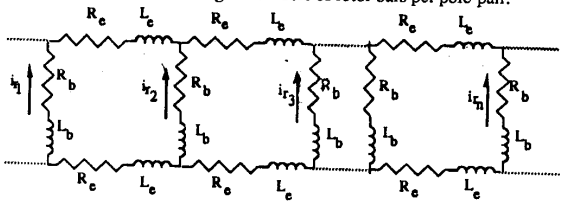

Figure 1 *Equivalent circuit of squirrel cage rotor.*

From Fig. 1 the voltage equations for the rotor loops are

$$V_r = R_r I_r + \frac{d\Lambda_r}{dt} \tag{14}$$

where

$$V_r = \left(v_1^r \; v_2^r \ldots\ldots\ldots\ldots v_n^r\right)^t$$

In case of a cage rotor $v_k^r = 0$; k=1,2,.....,n. The matrix R_r is n by n, symmetric and cyclic. The rows after the first can therefore be obtained by circular permutation. Each succeeding row is obtained from the previous row one step to the right with the last element inserted in the first column or,

$$R_r = \begin{pmatrix} 2(R_b+R_e) & -R_b & 0 & \ldots\ldots & -R_b \\ -R_b & 2(R_b+R_e) & -R_b & \ldots\ldots & 0 \\ \vdots & \vdots & \vdots & \ldots\ldots & \vdots \\ 0 & 0 & \ldots\ldots & 2(R_b+R_e) & -R_b \\ -R_b & 0 & \ldots\ldots & -R_b & 2(R_b+R_e) \end{pmatrix} \tag{15}$$

where R_e is the end ring resistance, and R_b rotor bar resistance. The rotor flux linkages Λ_r can be written as

$$\Lambda_r = L_{sr}^t I_s + L_{rr} I_r \tag{16}$$

where the matrix L_{sr}^t is the transpose of the matrix L_{sr} and the matrix L_{rr} is the n by n symmetric matrix

$$L_{rr} = \begin{pmatrix} L_{mr}+2(L_b+L_e) & L_{r_1r_2}-L_b & L_{r_1r_3} & \ldots\ldots & L_{r_1r_n}+L_b \\ L_{r_2r_1}-L_b & L_{mr}+2(L_b+L_e) & L_{r_2r_3}-L_b & \ldots\ldots & L_{r_2r_n} \\ L_{r_3r_1} & L_{r_3r_2}-L_b & L_{mr}+2(L_b+L_e) & \ldots\ldots & L_{r_3r_n} \\ \vdots & \vdots & \vdots & \ldots\ldots & \vdots \\ L_{r_nr_1}-L_b & L_{r_nr_2} & L_{r_nr_3} & \ldots\ldots & L_{mr}+2(L_b+L_e) \end{pmatrix} \tag{17}$$

In Eq. (17), L_{mr} is the magnetization inductance of each rotor loop, L_b the rotor bar leakage inductance, L_e the rotor end ring leakage inductance, $L_{r_i r_k}$ the mutual inductance between two rotor loops.

8. Calculation of Torque

The mechanical equation of motion depends upon the characteristics of the load which may differ widely from one application to the next . We will assume here, for simplicity, that the torque which opposes that produced by the machine consists only of an inertial torque and an external load torque which are known explicitly. In this case the mechanical equation of motion is simply

$$J\frac{d^2\theta_{rm}}{dt^2} + T_L = T_e \tag{18}$$

where θ_{rm} is the angular displacement of the rotor, T_L is the load torque, and T_e is the electromagnetic torque produced by the machine.

The electrical torque can be found from the magnetic coenergy W_{co} as

$$T_e = \left(\frac{\partial W_{co}}{\partial \theta_{rm}}\right) (I_s, I_r \text{ constant}) \tag{19}$$

In a linear magnetic system the coenergy is equal to the stored magnetic energy so that,

$$W_{co} = \frac{1}{2}\left(I_s^t \; I_r^t\right)\begin{pmatrix} L_{ss} & L_{sr} \\ L_{sr}^t & L_{rr} \end{pmatrix}\begin{pmatrix} I_s \\ I_r \end{pmatrix} \tag{20}$$

or

$$W_{co} = \frac{1}{2} I_s^t L_{ss} I_s + \frac{1}{2} I_s^t L_{sr} I_r + \frac{1}{2} I_r^t L_{sr}^t I_s + \frac{1}{2} I_r^t L_{rr} I_r \tag{21}$$

It is obvious that L_{ss} and L_{rr} contain only constant elements, so that Eq. (19) reduces immediately to

$$T_e = \frac{1}{2} I_s^t \frac{\partial L_{sr}}{\partial \theta_{rm}} I_r + \frac{1}{2} I_r^t \frac{\partial L_{sr}^t}{\partial \theta_{rm}} I_s \tag{22}$$

Since T_e is a scalar, each of the two terms comprising T_e must be a scalar. Because the transpose of a scalar is clearly the scalar itself, it must be true that the second term must equal its transpose, or

$$I_r^t \frac{\partial L_{sr}^t}{\partial \theta_{rm}} I_s = \left(I_r^t \frac{\partial L_{sr}^t}{\partial \theta_{rm}} I_s\right)^t \tag{23}$$

From matrix algebra

$$\left(A^t \; B^t \; C\right)^t = C^t \; B \; A$$

so that

$$I_r^t \frac{\partial L_{sr}^t}{\partial \theta_{rm}} I_s = I_s^t \frac{\partial L_{sr}}{\partial \theta_{rm}} I_r \tag{24}$$

Hence the first term of Eq. (22) is equal to the second. The torque equation reduces to the final form

$$T_e = I_s^t \frac{\partial L_{sr}}{\partial \theta_{rm}} I_r \tag{25}$$

Thus far, it has been assumed, for simplicity, that the machine has only two poles. In general, let P denote the number of motor poles. It is clear that any inductance which is a function of angular displacement undergoes P/2 complete cycles as θ_{rm} varies from 0 to 2π. That is

$$\theta_r = \frac{P}{2}\theta_{rm} \tag{26}$$

The angle θ_r is called the rotor displacement in electrical radians. In terms of θ_r , the torque is clearly

$$T_e = \frac{P}{2} I_s^t \frac{\partial L_{sr}}{\partial \theta_r} I_r \tag{27}$$

Finally Eq. (18) in terms of θ_r is

$$\frac{2}{P} J \frac{d^2\theta_r}{dt^2} + T_L = T_e \tag{28}$$

9. Calculation of Terminal Voltages

In matrix form the stator voltage equation is given by Eq. (1). Substituting Eq. (13) in (1) yields

$$V_s = R_s I_s + L_{ss}\frac{dI_s}{dt} + \omega_{rm}\frac{dL_{sr}}{d\theta_{rm}} I_r + L_{sr}\frac{dI_r}{dt} \tag{29}$$

In the above equation the components are 1) resistive drop, 2) the transformer voltages arising from time varying stator currents, 3) the speed voltages which appear due to coupling between stator phases and rotor bars, and 4) the transformer voltages resulting from time variation in rotor bars current. Since it will be assumed that the machine is excited from a current source rather than a voltage source, it is convenient to express Eq. (29) in a slightly different form.

Taking the derivative of Eq. (16) with respect to time and substituting for the derivative of the mutual inductances from Eq. (12) results in

$$\frac{d\Lambda_r}{dt} = \omega_{rm}\frac{dL_{sr}^{t}}{d\theta_{rm}} I_s + L_{sr}^{t}\frac{dI_s}{dt} + L_{rr}\frac{dI_r}{dt} \qquad (30)$$

substituting this result in Eq. (14) and rearranging yields

$$\frac{dI_r}{dt} = -L_{rr}^{-1} R_r I_r - L_{rr}^{-1} L_{sr}^{t}\frac{dI_s}{dt} - \omega_{rm} L_{rr}^{-1}\frac{dL_{sr}^{t}}{d\theta_{rm}} I_s \qquad (31)$$

From Eqs. (1), (13), and (31) we can now find the terminal voltages in terms of only the stator current and its derivative (considered as inputs) and the rotor current state variables. The result is expressed as

$$V_s = (R_s - \omega_{rm} L_{sr} L_{rr}^{-1}\frac{dL_{sr}^{t}}{d\theta_{rm}})I_s + (L_{ss} - L_{sr} L_{rr}^{-1} L_{sr}^{t})\frac{dI_s}{dt}$$

$$(L_{sr} L_{rr}^{-1} R_r - \omega_{rm}\frac{dL_{sr}}{d\theta_{rm}})I_r \qquad (32)$$

10. Calculation of Inductances of a Concentrated Winding Induction Machine

All of the relevant inductances for the concentrated winding induction machine can be calculated using the winding function method given in [10]. For purposes of illustration the technique is best described by considering an elementary 3 phase, 2 pole induction machine having only 2 rotor bars per pole given in Fig. 2. The winding function for each stator coil is shown in Fig. 3(a) and the winding function for each rotor loop is depicted in Fig. 3(b).

The magnetizing inductance for each stator coil is given by

$$L_{ma} = L_{mb} = L_{mc} = \frac{\mu_0 rL}{g}\frac{\pi N^2}{2} \qquad (33)$$

where r is the average value of the stator inner and rotor outer radius, g is the air-gap, and L is the length of the coil.

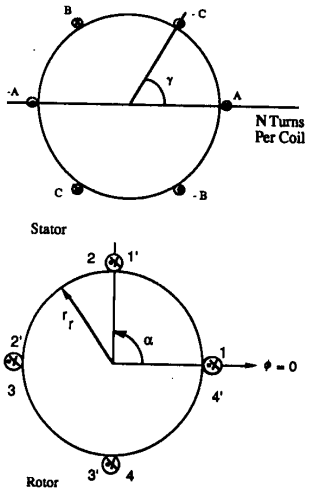

Figure 2 *The 3-phase, 2-pole induction machine having two rotor bars per pole.*

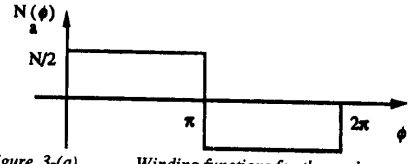

Figure 3-(a) *Winding functions for three-phase, two-pole concentrated winding induction motor.*

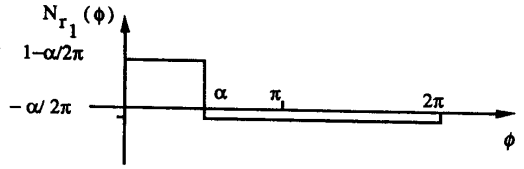

Figure 3-(b) *Winding functions for each rotor loop of Figure 2*

Assume γ is the angle between two stator slots in radians which obviously in this case is π/3. The mutual inductances between stator phases are

$$L_{ab} = L_{ba} = \frac{\mu_0 rL}{g}\frac{\pi N^2}{2}\left(1 - \frac{4\gamma}{\pi}\right) \qquad (34)$$

$$L_{bc} = L_{cb} = \frac{\mu_0 rL}{g}\frac{\pi N^2}{2}\left(-1 + \frac{2\gamma}{\pi}\right) \qquad (35)$$

$$L_{ac} = L_{ca} = \frac{\mu_0 rL}{g}\frac{\pi N^2}{2}\left(-1 + \frac{2\gamma}{\pi}\right) \qquad (36)$$

where if we substitute for γ=π/3 we obtain the usual result,

$$L_{ab} = L_{ba} = L_{bc} = L_{cb} = L_{ac} = L_{ca} \qquad (37)$$

Equation (37) expresses the result of assuming that all phases are placed equidistant with respect to each other.

Assume now that α is the angle between two rotor bars in radians. In Fig. 2, α is equal to π/2. The magnetizing inductance of the rotor loop is given by

$$L_{mr} = \frac{\mu_0 rL}{g}\alpha\left(1 - \frac{\alpha}{2\pi}\right) \qquad (38)$$

The mutual inductance between any two rotor loops is

$$L_{r_j r_k} = \frac{\mu_0 rL}{g}\left(-\frac{\alpha^2}{2\pi}\right) \qquad (39)$$

Finally the mutual inductance between stator phase A and rotor loop 1 is depicted in Fig. 4 and given by

$$L_{ar_1} = \frac{\mu_0 rL}{g}\frac{N}{2}\alpha \qquad 0 \le \theta_{rm} < \pi - \alpha$$

$$L_{ar_1} = \frac{\mu_0 rL}{g}\frac{N}{2}(2\pi - 2\theta_{rm} - \alpha) \qquad \pi - \alpha \le \theta_{rm} < \pi$$

$$L_{ar_1} = -\frac{\mu_0 rL}{g}\frac{N}{2}\alpha \qquad \pi \le \theta_{rm} < 2\pi - \alpha$$

$$L_{ar_1} = \frac{\mu_0 rL}{g}\frac{N}{2}(4\pi - 2\theta_{rm} - \alpha) \qquad 2\pi - \alpha \le \theta_{rm} < 2\pi \qquad (40)$$

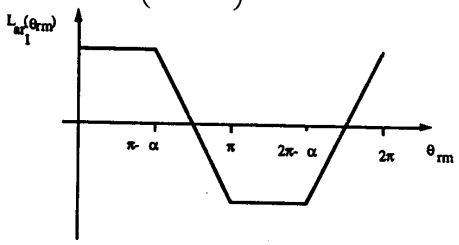

Figure 4 *The mutual inductance between stator phase a and rotor loop r_1.*

11. Simulation Results

To verify the model developed previously a three phase, conventionally wound with a pitch of 8/9, 4 -pole, 7.5 horsepower induction motor has been simulated. The stator of this machine has 36 slots and the rotor has 28 slots and is not skewed. The machine operates from a balanced sinusoidal supply. Figure 5 presents the instantaneous electromagnetic torque with respect to time during start up. It can be noted that the effects of space harmonics are translated into torque pulsations. It should be mentioned that since the winding functions are modeled with sharp edges the effect of space harmonics are rather profound. Variation of speed versus time is depicted in Fig. 6 which again the effect of space harmonics at the starting is clear. Finally Fig. 7 demonestrate the variation of average torque with respect to speed representing a hook at one-seventh of synchronous speed in the torque-speed characteristic which is in complete agreement with the method given by Kron in [11] as a result of space harmonics.

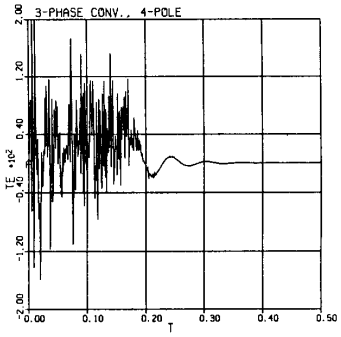

Figure 5 *Instantaneous electromagnetic torque- Free acceleration.*

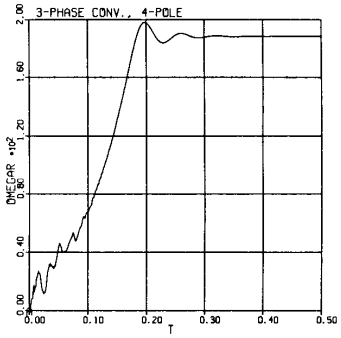

Figure 6 *Shaft speed variation- Free acceleration.*

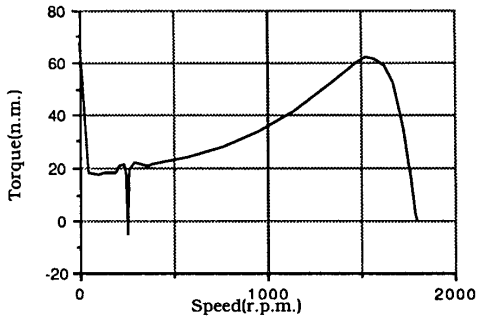

Figure 7 *Average torque - speed curve indicating a hook at one-seventh of synchronous speed.*

12. Conclusion

The equations describing the performance of multiphase induction machines during the transient as well as steady state behavior including the computation of all machine inductances are derived. In deriving these equations the space harmonics have been specifically included. Equations for calculation of terminal voltages and electromagnetic torque have also been modified to account for non sinusoidal air gap flux distributions. Finally a conventional 3 phase induction motor including the effect of space harmonics has been simulated

References

[1] Turnbull, F.G., "Selected Harmonic Reduction in Static dc-ac Inverters," IEEE Trans. Commun. Electron, vol. 83, 1964, pp. 374-378.

[2] Patel, H.S., and Hoft, R.G., "Generalized Techniques of Harmonic Elimination and Voltage Control in Thyristor Inverters: Part 1- Harmonic Elimination," IEEE Trans. Ind. Appl., vol. IA-9, No. 3, 1973, pp. 310-317.

[3] Lipo, T.A., and Wang, F.X., "Design and Performance of a Converter Optimized AC Machine," IEEE Trans. Ind. Appl. vol. IA-20, No. 4, July/August, 1984, pp. 834-844.

[4] Wang, F.X. and Lipo, T.A., "Analysis and Steady State Behavior of an Optimized AC Converter Machine," IEEE Trans. Power App. Syst., vol. PAS-102, pp. 2734-2742, Aug. 1983.

[5] Wang, F.X. and Zhang, B.Y. "Waveform Optimization Design of an AC Converter Machine," IEEE Trans. Ind. Appl., vol 25, No. 3, pp. 436-440, May/June 1989.

[6] Dente, J.G., "Squirrel-cage Induction Motor with Electronic Commutation," International Conf. on Evolution and Modern Aspect of Induction Machines, July 8-11, 1986, Torino, Italy, pp. 596-599.

[7] Gosden, D.F., "An Inverter-Fed Squirrel Cage Induction Motor with Quasi-Rectangular Flux Distribution," Electric Energy Conf., October 6-9, 1987, Adelaide, Australia, pp. 240-245.

[8] Weh, H., and Schroder, U., "Static Inverter Concepts for Multiphase Machines with Square-wave Current Field Distributions," First European Conference on Power Electronics and Applications, Brussels, 16-18 October, 1985, pp. 1.147-1.152.

[9] Fudeh, H.R., and Ong, C.M., "Modeling and Analysis of Induction Machines Containing Space Harmonics," Part 1,2, and 3, IEEE Trans. Power App. and Sys., Vol. PAS-102, No.8, August 1983, pp. 2608-2628.

[10] Lipo, T.A.,"Theory and Control of Synchronous Machines," University of Wisconsin-Madison, 1987.

[11] Kron, G.,"Induction Motor Slot Combinations, Rules to Predetermine Crawling, Vibration, Noise, and Hooks in the Speed-Torque Curve," AIEE, Vol. 50, June 1931, pp. 757-768